Research on seismic performance of corrugated web rigid structures

Cao Huimin

(Xi'an Traffic Engineering Institute, Xi·an710072, China)

Abstract: Corrugated web steel refers to the wavy steel along the length direction, which is widely used in beams, columns, walls, and other parts of the building structure, playing the role of connection and support. The wavy or corrugated shape of the web improves the shear instability and out-of-plane stiffness of the web to a certain extent. However, although H-shaped steel members with corrugated webs have the advantages of high strength, large stiffness, lightweight, and convenient construction, the relevant regulations point out that this kind of members can only be used for lower intensity or can be applied to higher intensity only when certain conditions are satisfied. one of the important conditions is that the ratio of the product of the design value of axial force with seismic action to the design value of flange section area and tensile strength of steel does not exceed 0.4. In this regard, this paper will further explore the seismic characteristics and applicable intensity of corrugated steel structure under earthquake through large-scale finite element ABAQUS simulation, observe the dynamic characteristics and failure of corrugated rigid frame structure by elastic-plastic time-history analysis method, and observe the plastic deformation characteristics of steel beam members under low cyclic load by hysteretic analysis method. The study shows that when the beam span and design are reasonable. The beam of corrugated web rigid frame structure can still be used in the area of high intensity above 7 degrees when the axial compression ratio is 0.5.

Keywords: corrugated web; Intensity; Hysteresis characteristics; TAxial compression ratio

Introduction：

Green building comprehensively implements the concept of green, environmental protection, and energy saving in project construction and construction, and maintains the characteristics of sustainable development, while the development of prefabricated steel structures effectively promotes the development of green building.[1]

Corrugated steel profile is a new type of green building steel developed in recent decades. Due to the accessibility of materials, components can be cut and assembled at the construction site, no waste of production, reduced transportation costs, and other advantages such as the possibility of selecting cross-sections according to load make its research continue[2]. With the recent in-depth exploration of researchers, the static research of corrugated steel profiles has been relatively mature, and the dynamic research has gradually increased. In terms of bridges, Jiang Lizhong and others verified through experiments that the load-displacement hysteresis loop of steel-concrete composite box girders with corrugated webs is full and has no obvious pinch phenomenon under low cyclic loading, and has good seismic performance [3]. In this paper, according to the principle of equal shear

capacity of box girder section, the finite element models of corrugated steel web continuous rigid frame bridge and corresponding concrete web continuous rigid frame bridge are established, and their dynamic characteristics and seismic performance are compared and analyzed. the study shows that under the earthquake, the internal force of the low pier and the shear force at the top of the high pier of the corrugated steel web rigid frame bridge are less than those of the concrete web rigid frame bridge. While the bending moment at the top of the high pier and the internal force at the bottom of the pier are greater than the latter[4]. Through the analysis of mechanical formula, Li Pengfei proved that the use of hollow piers not only has a small weight but also can effectively improve the torsional performance and lateral push stiffness of the superstructure of continuous rigid frame bridges with corrugated steel webs. Hollow piers have great advantages when designing continuous rigid frame box girder bridges with corrugated steel webs. Architecture: Wanyu analyzed the seismic behavior of the H-section steel cantilever beam and frame with a corrugated web through the ABAQUS finite element model[6]. Peng Jiacheng developed a kind of corrugated web damper with good seismic performance through experiments, which further expanded the application field of corrugated steel[7]. Xingyu Mou et al proposed a new type of composite shear wall composed of a corrugated concrete-filled steel tubular column frame and filled corrugated steel plate, and proved that the composite structure has good seismic performance through numerical analysis and experiments. Combined with the actual investigation, although the corrugated web profile has many advantages, it is still not widely used in China because of its complex production process and seismic performance. Therefore, the research of corrugated steel in the seismic field of industrial and civil buildings is of great significance [11].

In this study, the combination of dynamics and quasi-statics is used for simulation and analysis. through the method of time history analysis of rigid frame and hysteretic analysis of steel beam[12], the ratio of the product of axial force design value of corrugated steel member with flange section area and steel tensile strength design value of corrugated steel member is further analyzed, which provides a theoretical basis for this member to be used in a high-intensity seismic area.

1 model and analytical hypothesist

1.1 Analytical model and parameters

The model of this paper is created by ABAQUS finite element software, and the S4R shell element is adopted. The constitutive model of steel is shown in Fig.1-1, and the material parameters are shown in Tab.1-1. Figures 1-2 and Tab.1-2 are the zigzag parameters of the web used in this paper.

Tab. 1-1Material Parameters

Steel products	Elastic modulus	Density	Poisson 's ratio	Design value of tensile strength
Q345	$2.06\times10^{11}N/m^2$	7850kg/ m^3	0.28	$310N/mm^2$

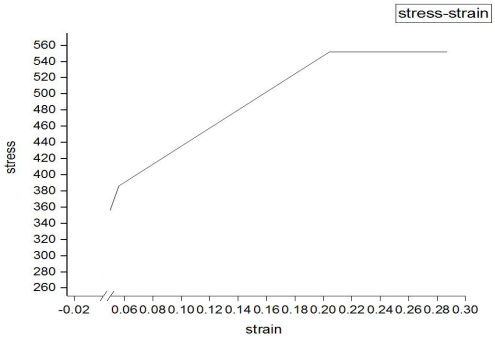

Fig. 1-1 Material Constitutive Model

Tab.1-2 Comparison Tab.of Geometric Parameters of Component

Angle （°）	Wave length （mm）	Wave height (mm)	Flange thickness-to-width ratio	Thick-ness (mm)	Web height （mm）
45	240	25	0.05	2	520

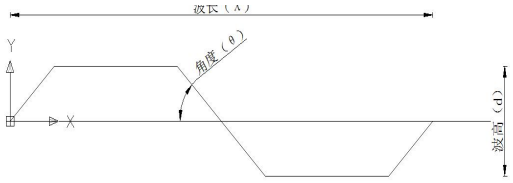

Fig. 1-2 Web plate bending parameters

Model an in Fig.1-3 is a corrugated rigid frame structure with zero slopes of the roof ridge. the lengths of beam members are 6m, 12m, 18m, and 24m respectively, and the column heights are all 6m. The node is just a knot. X, Y, and Z directions are column height direction, perpendicular to beam axis direction and rigid frame span direction respectively; model b is the model of ordinary rigid frame beam members, and the hysteretic characteristics of corrugated steel beam members are observed by loading low cycle reciprocating load.

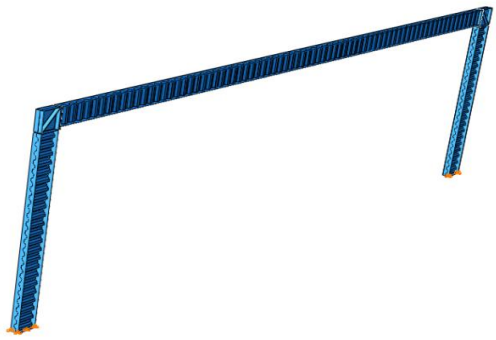

Model a Rigid frame structure model

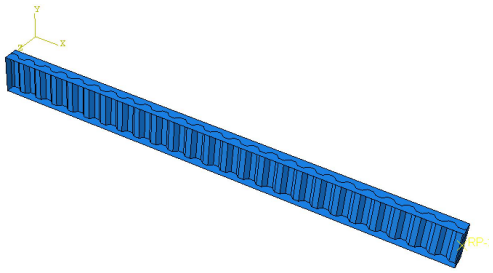

Model b Steel beam structure model

Fig.1-3 Model diagram

1.2 Analytical assumptions

It is assumed that the connections between the rigid frame and the member nodes and supports are rigid in the ideal state; it is assumed that the rigid frame structural beam only supports the

profiled steel roof and cold-formed steel purlin; it is assumed that the structure is subjected to force in the ideal state.

2 dynamic analysis of rigid frame structure

2.1 Modal analysis

Taking the rigid frame with a span of 12 meters as an example, the modal analysis of the structure is carried out, and each mode is shown in Fig.2-1.

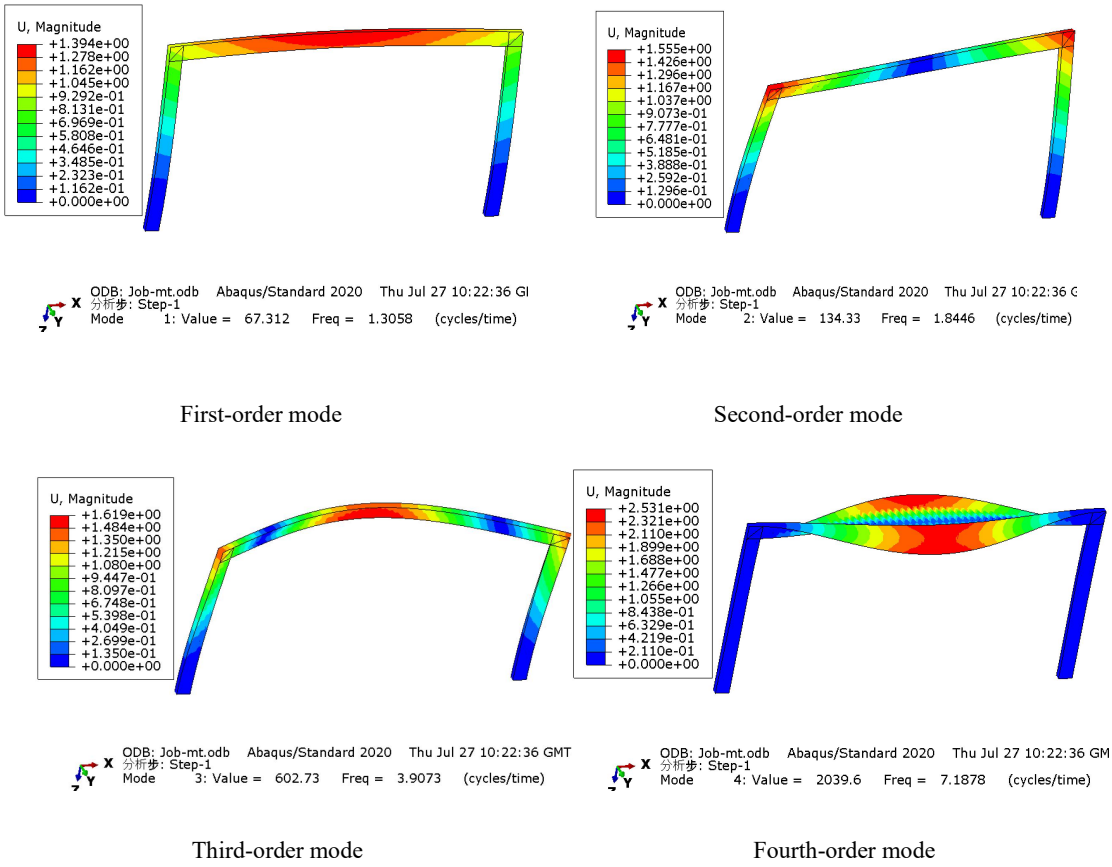

Fig. 2-1 Modal Analysis Diagram

In this model, the first four modes are extracted by the subspace iteration method, in which the first frequency is 1.3058HZ, that is, the period of the model is 0.74s. There is little difference between the manual calculation and the software results obtained from the calculation formula $\omega = \sqrt{\frac{K}{M}}$, which shows that the structural model is correct and available.

2.2 time history analysis

In the time-history analysis, the beam is simulated as a compression-bending member by applying a pair of eccentric forces, where the axial compression ratio is controlled to be 0.4 and 0.5 respectively, and the formula is used to calculate the axial compression ratio. $n = N / (f * A_f)$,

Among them, *T*he axial pressure value, A_f -the net cross-sectional area of the flange, and f -the design value of steel tensile strength.

2.2.1 amplitude modulation of seismic wave

The constraint Ux, UR1, UR2, UR3 at the bottom of the column is zero, and Uy and Uz apply EL-Centro seismic wave, through the formula. $a_0(t_i)=\frac{a_{0,\max}}{a_m}a(t_i)$ carry out amplitude modulation， Now take the rare occurrence of EL-Centro wave of degree 7, that is, the peak value of seismic wave as 2.20m/s2, as an example， By amplitude modulation[13]， This is shown in Fig.3-1.

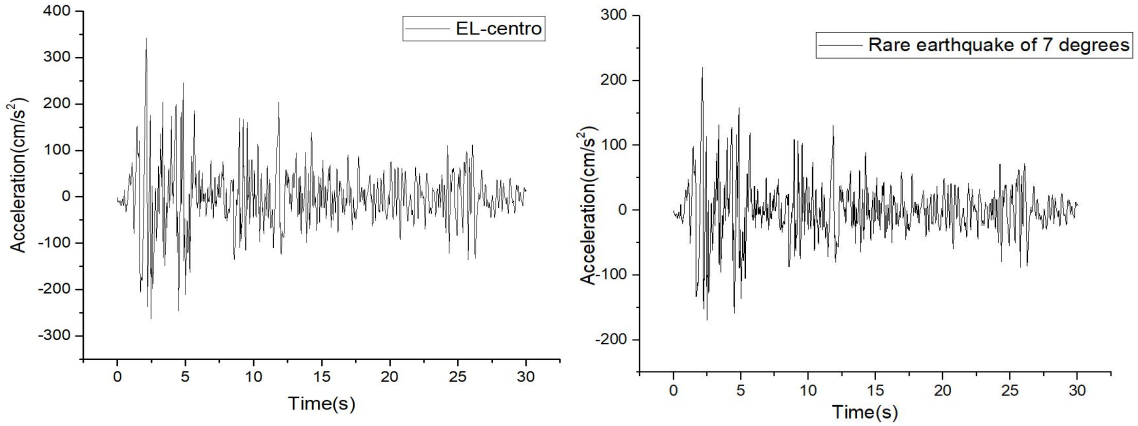

（a） **Before the *EL-Centro* Amplitude Modulation**　　（b） **After the *EL-Centro* Amplitude Modulation**

Fig.3-1 Comparison of EL Centro Wave before and after Amplitude Modulation

2.2.2 Basis for Analysis

According to the Stipulate of the the 《Technical Specification for Steel Structures of Lightweight Buildings with Portal Frames》（*GB51022:2015*）[12]3.3.1： A single-layer portal steel frame, without crane and light steel wallboard, the displacement of the top of the column is not greater than H/ 60, that is, the interlayer displacement angle is not more than 0.017.

According to the Stipulate of the the 《Technical Specification for Steel Structures of Lightweight Buildings with Portal Frames》（*GB51022:2015*）[12]3.3.2：For inclined beams of portal frames, when only profiled steel roofs and cold-formed steel purlins are supported, the limit of deflection of members is L /180, where L is the full-span length.

2.2.3 Result analysis

1. Comparative analysis when the axial compression ratio is 0.4 and 0.5 under earthquake:

The eccentric load is applied to the beam of the rigid frame structure, so that the member is under the action of the set axial compression ratio, and the seismic wave is applied under the rare

earthquake at the bottom of the rigid frame column. Firstly, the stress and failure of the structure under an earthquake are compared and analyzed when the axial compression ratio is 0.4 and the axial compression ratio is 0.5.

Tab.3-1 Variables Corresponding to Different Seismic Wave

Beam span	Axial compression ratio	Wave peak value	220	310	400	510	620
6m	0.4	(Interlayer displacement) $_{max}$	39.29	54.91	70	89.60	**108.61**
		(Interlayer displacement angle) $_{max}$	0.0065	0.0092	0.0117	0.0149	**0.0181**
		(Mid-span deflection)$_{max}$	5.30	5.46	5.60	5.76	5.90
	0.5	(Interlayer displacement) $_{max}$	39.63	55.20	70.45	89.34	**108.67**
		(Interlayer displacement angle) $_{max}$	0.0066	0.0092	0.0117	0.0149	**0.0181**
		(Mid-span deflection)$_{max}$	6.65	6.68	6.81	7.10	7.14
12m	0.4	(Interlayer displacement) $_{max}$	40.79	56.36	72.03	91.21	**109.89**
		(Interlayer displacement angle) $_{max}$	0.0068	0.0094	0.0120	0.0152	**0.0183**
		(Mid-span deflection)$_{max}$	13.51	13.62	13.79	13.92	14.01
	0.5	(Interlayer displacement) $_{max}$	41.30	56.51	72.66	91.86	**111.04**
		(Interlayer displacement angle) $_{max}$	0.0069	0.0094	0.0121	0.0153	**0.0185**
		(Mid-span deflection)$_{max}$	16.57	16.72	16.80	16.91	17.07
18m	0.4	(Interlayer displacement) $_{max}$	31.65	42.57	46.57	58.31	81.41
		(Interlayer displacement angle) $_{max}$	0.0053	0.0071	0.0078	0.0097	0.0136
		(Mid-span deflection)$_{max}$	24.98	24.99	25.12	25.68	25.82
	0.5	(Interlayer displacement) $_{max}$	32.70	43.20	54.79	68.57	82.26
		(Interlayer displacement angle) $_{max}$	0.0055	0.0072	0.0091	0.0114	0.0137
		(Mid-span deflection)$_{max}$	30.24	30.33	30.61	30.94	31.10
24m	0.4	(Interlayer displacement) $_{max}$	31.20	41.82	52.35	65.33	78.57
		(Interlayer displacement angle) $_{max}$	0.0052	0.0070	0.0087	0.0109	0.0131
		(Mid-span deflection)$_{max}$	42.47	40.76	41.02	41.27	41.61
	0.5	(Interlayer displacement) $_{max}$	32.48	43.45	53.5	66.40	79.36
		(Interlayer displacement angle) $_{max}$	0.0054	0.0072	0.0089	0.0111	0.0132
		(Mid-span deflection)$_{max}$	50.31	48.03	50.61	50.98	50.14

Note: the peak unit of seismic wave is cm/s^2, and the unit of displacement and deflection is mm.

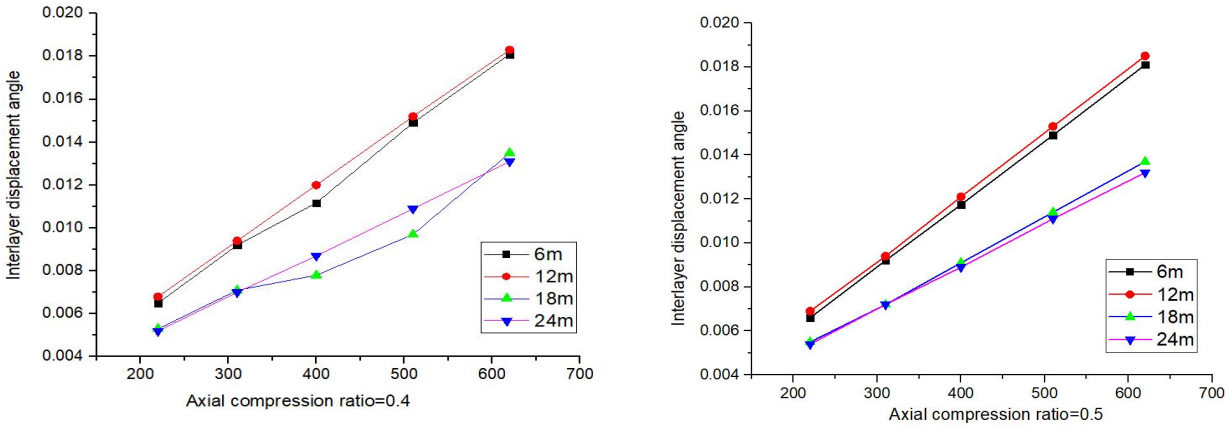

Fig.3-2 Maximum Interstory Displacement Angle

As can be seen in Fig.3-2 and Fig.3-3, no matter how much the beam span is, the inter-story displacement and inter-story displacement angle are not affected by the axial compression ratio, and their values increase with the increase of seismic wave intensity.

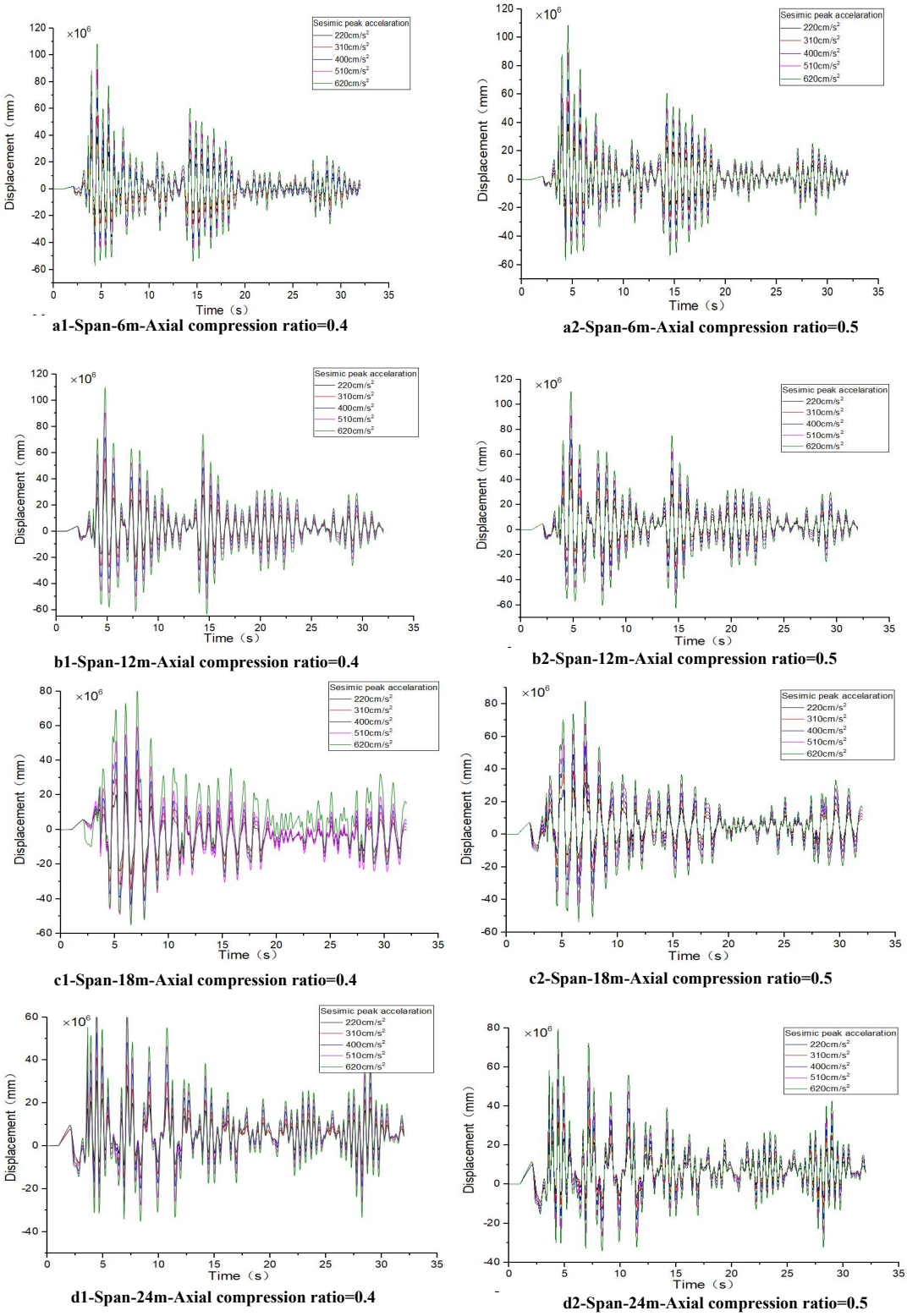

a1-Span-6m-Axial compression ratio=0.4

a2-Span-6m-Axial compression ratio=0.5

b1-Span-12m-Axial compression ratio=0.4

b2-Span-12m-Axial compression ratio=0.5

c1-Span-18m-Axial compression ratio=0.4

c2-Span-18m-Axial compression ratio=0.5

d1-Span-24m-Axial compression ratio=0.4

d2-Span-24m-Axial compression ratio=0.5

Fig.3-3 Time history curves of different spans and axial compression ratios

The greater the earthquake acceleration, the greater the damage to the structure. Here, we tend to observe the force cloud diagram of the member when the intensity is 9 degrees. The cloud diagram in Tab.3-2 shows that the member does not reach the yield strength when the axial compression ratio is 0.4 and 0.5, And the stress value decreases with the increase of span. The maximum internal force of the structure is 647.7kN, and the corresponding axial compression ratio is about 0.52. the maximum stress is that 224.9MPa does not reach the yield stress of the structural material, so the structure is not damaged.

Tab.3-2 Cloud Chart of Different Spans and Axial Compression Ratios

Span	The axial compression ratio is 0.4	The axial compression ratio is 0.5
6m	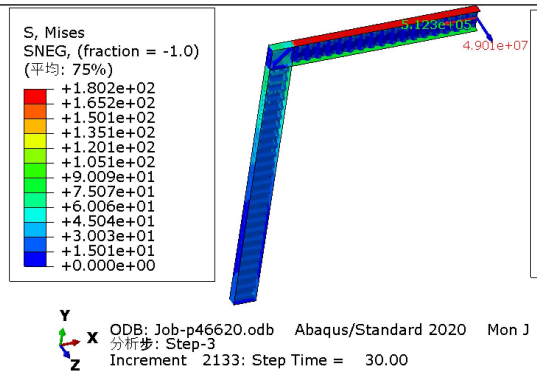	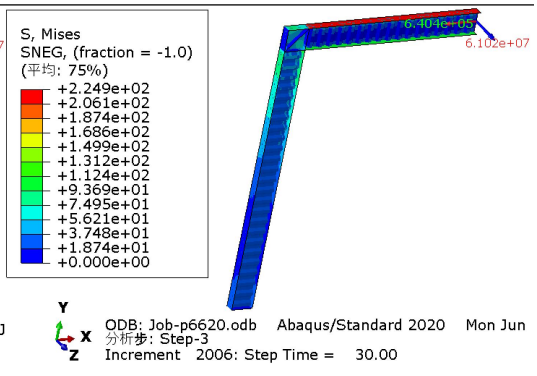
12m	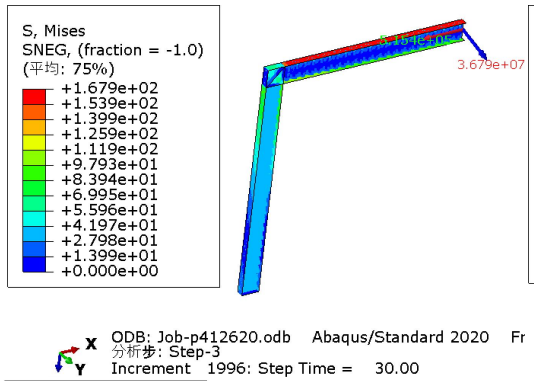	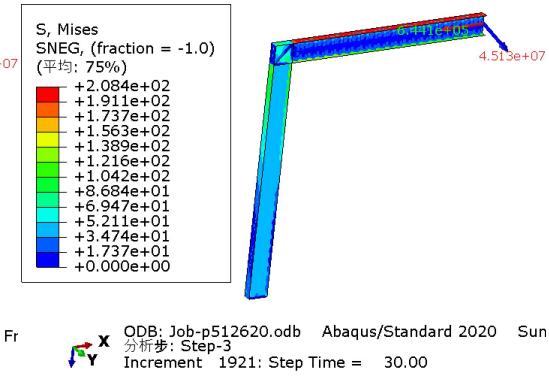
18m	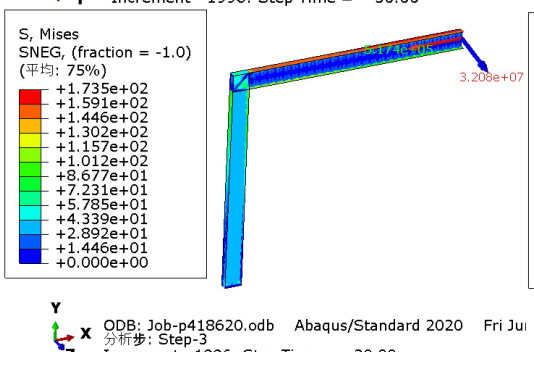	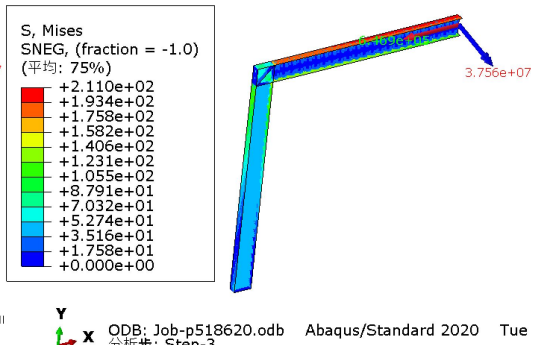

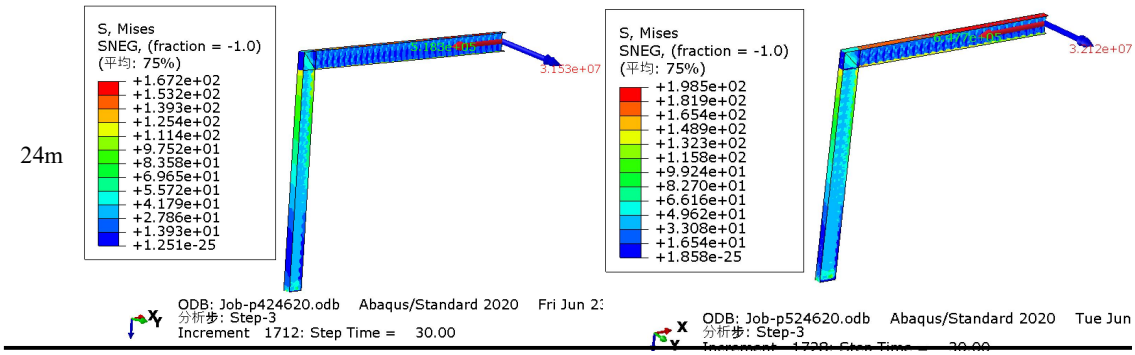

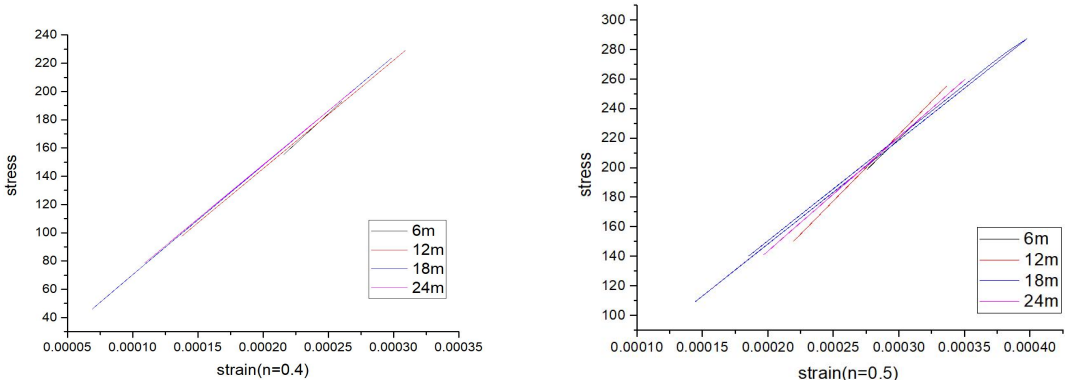

Fig. 3-4 Stress-strain curves of different spans and different axial compression ratios

From the stress-strain curves of different spans and different axial compression ratios in Fig.3-4, we can see that no matter whether the axial compression ratio is 0.4 or 0.5, the stress-strain curves are in the elastic stage when the beam span is 6-24m, which can better withstand the external load and earthquake force.

2. When the axial compression ratio is 0.6, 0.7 and 0.8

Section 3.1 shows that when the beam span is 6m and 12m, the limit of interlaminar displacement can not be met under a 9-degree earthquake, which is mainly because the small span-height ratio is relatively more prone to brittle shear failure in the earthquake. With the increase of span-height ratio, its mechanical behavior is gradually close to that of conventional frame beams, and the seismic performance will become better [15-19]. Therefore, it can be inferred that when the axial compression ratio is larger. 6m and 12m are still not enough for 9-degree rare earthquakes. To further observe the limit value of the axial compression ratio that can be reached by a corrugated rigid frame, a similar method will be used to analyze the damage of the structure under 9-degree rare earthquakes when the axial compression ratio is 0.6, 0.7, and 0.8.

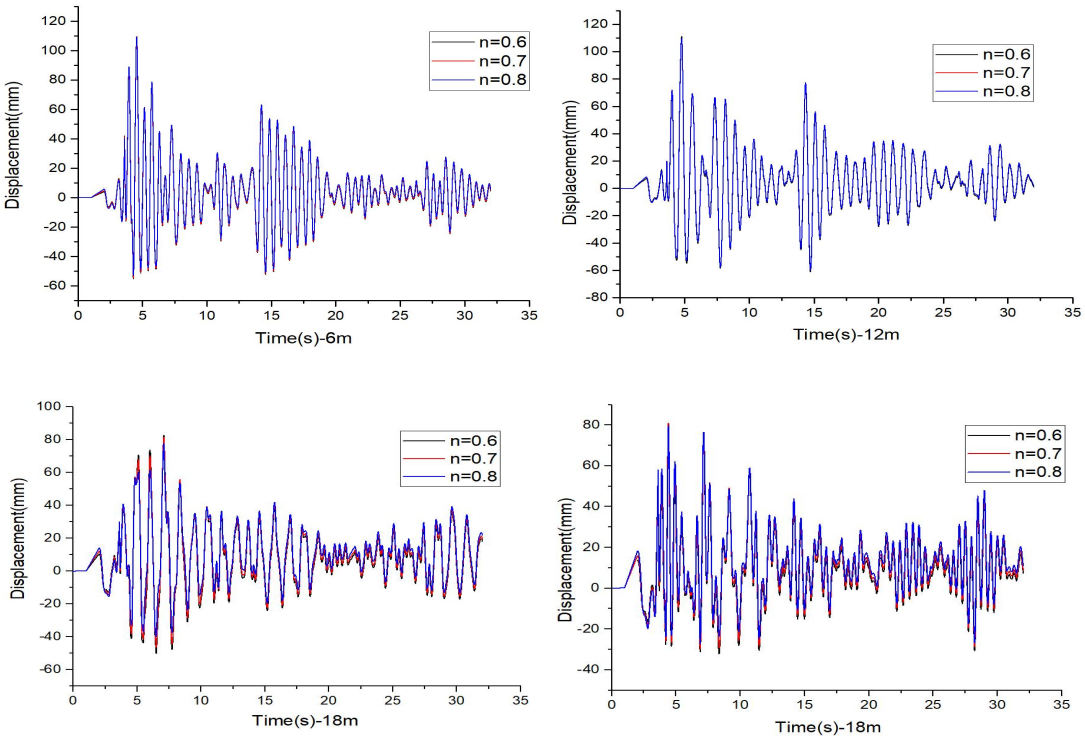

Fig. 3-6 Interlayer displacement curves with different spans and different axial compression ratios

From the《Technical Specification for Steel Structures of Lightweight Buildings with Portal Frames》（*GB51022:2015*） and the inter-story displacement curve of Fig.3-6, it can be seen that under the action of 9 degrees of rare earthquake, when the beam span is 6m and 12m, the inter-story displacement can not meet the requirements of the code, while when the span is 18m and 24m, it can meet the requirements. It can be seen from Tab.3-3 that the deflection meets the requirements of the code. This conclusion is consistent when the coaxial compression ratio is 0.4 and 0.5.

Tab. 3-3 deflection at different spans and axial compression ratios

Beam span / n	6m	12m	18m	24m
0.6	**8.4**	**20.23**	**37.03**	**59.57**
0.7	**9.4**	**22.7**	**44.75**	**68.20**
0.8	**12.48**	**28.94**	**60.00**	**84.50**
限值	**33.33**	**66.67**	**100**	**133.33**

The stress-strain curve in Fig.3-5 shows that the stress-strain curve shows a certain hysteretic characteristic when the axial compression ratio increases, and the greater the axial compression ratio, the more obvious the hysteretic characteristic, indicating that the rigid frame beam has a plastic deformation with the increase of axial compression ratio. and with the increase of axial compression ratio, the plastic deformation also increases.

To fully ensure that the rigid frame structure has better seismic characteristics, the structure should be in the elastic stress stage as far as possible. Therefore, combined with the above conclusion, it can be known that the rigid frame structure still has good seismic characteristics when the axial compression ratio is 0.5.

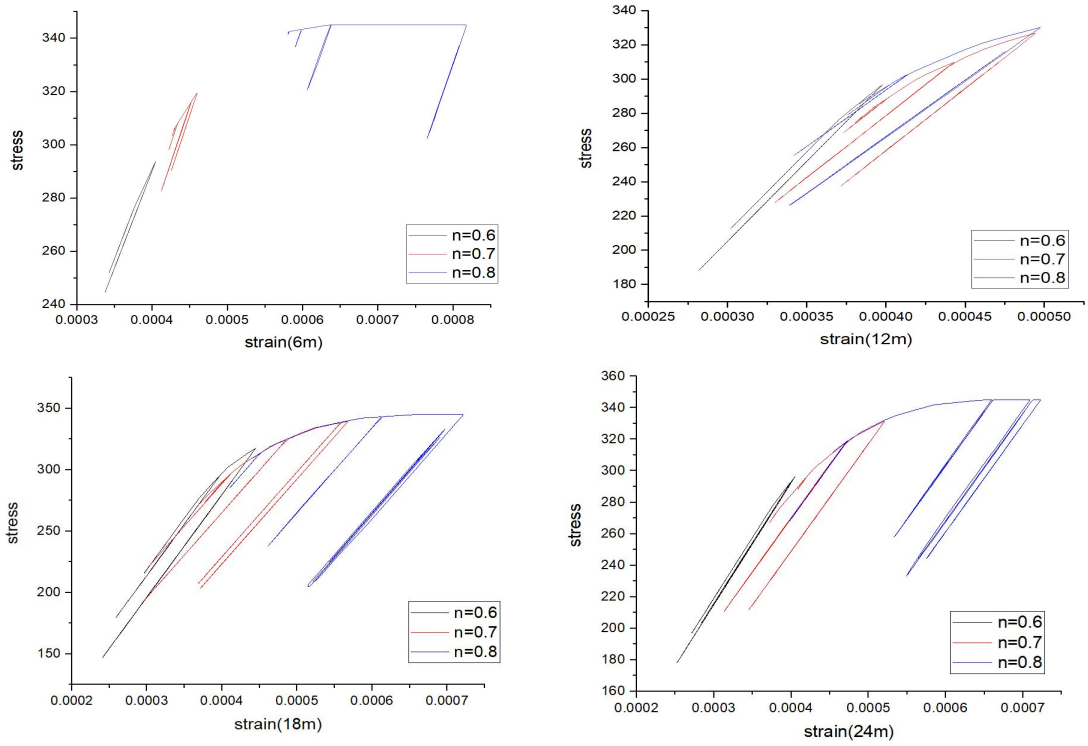

Fig. 3-5 stress-strain curves of different spans

3. Quasi-static analysis

In the quasi-static hysteretic analysis part, one end is completely consolidated, that is, all six degrees of freedom are zero, and the simplified model loaded at the other end applies the displacement amplitude of the vertical beam direction at the loading end when the axial compression ratio is 0.4 and 0.5 respectively. The displacement starts from 0mm, every 4 s is a circle and loads to 180 mm step by step. At the same time, the corresponding time length [20] [21] is set in the analysis step, and the loading system is shown in Fig.3-4.

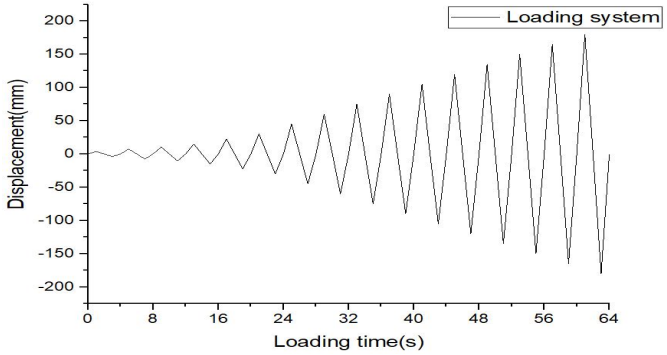

Fig. 3-4 Loading System

From the hysteretic curve and Mises cloud diagram of Tab.3-4, it can be seen that the change in axial compression ratio has little influence on the hysteretic loop. When the beam spans 6m, the hysteretic curve is the fullest, slightly pinched, and the energy dissipation capacity is the strongest. The skeleton curve has experienced three stages of elasticity, elastoplasticity, and plasticity [22], and the two ends of the beam have reached the yield limit.

When the beam span is 12m, the hysteretic curve has been pinched, and the beam appears a certain degree of torsion under the action of displacement loading. at this time, the failure point of the steel beam is no longer concentrated at the end of the beam, but the local buckling occurs at the torsion point.

As can be seen from Tab.3-4, with the increase of the shear-span ratio, the area surrounded by the hysteretic loop gradually decreases, the hysteretic curve pinches and slips seriously, the external force required by the same displacement becomes smaller, and the energy dissipation becomes smaller [23]. The torsional slip of the member is serious at 18m, while the member with a 24m span is almost in elastic deformation, but the energy dissipation decreases obviously.

To sum up, it can be concluded that the hysteretic analysis load that the structure can bear under the action of a specific axial compression ratio decreases with the increase of the span, and the axial compression ratio has little effect on the hysteretic performance, but the effect of low cyclic load can still be used as a reference for seismic analysis.

Tab.3-3 Time Delay Loop Curve and Cloud Chart for Different Axial Pressure Ratios

	Hysteretic curve	Mises cloud picture
6m	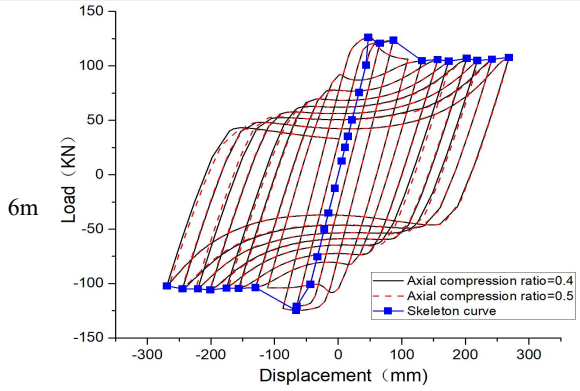	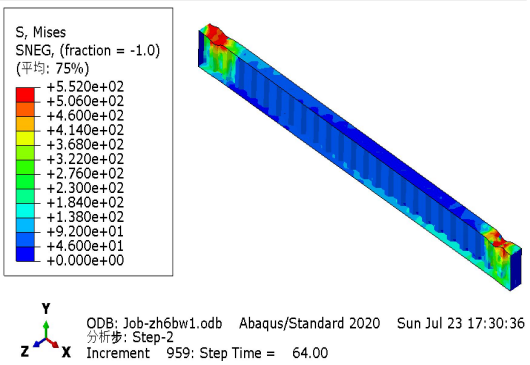
12m	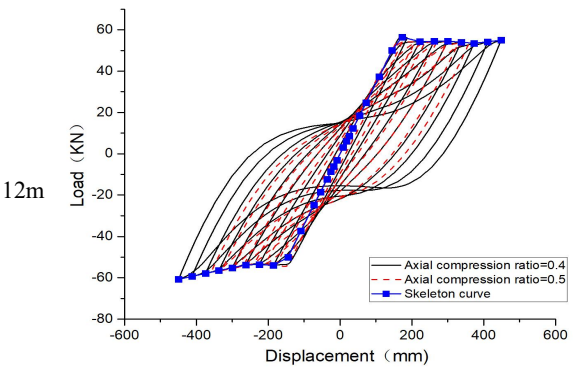	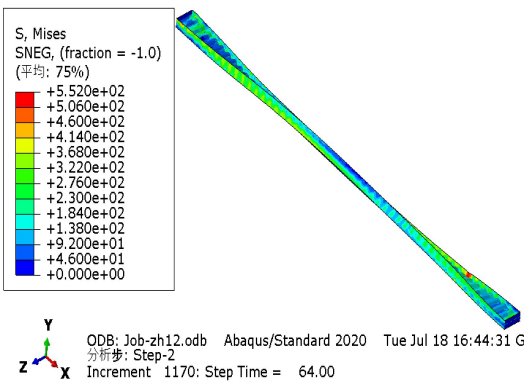

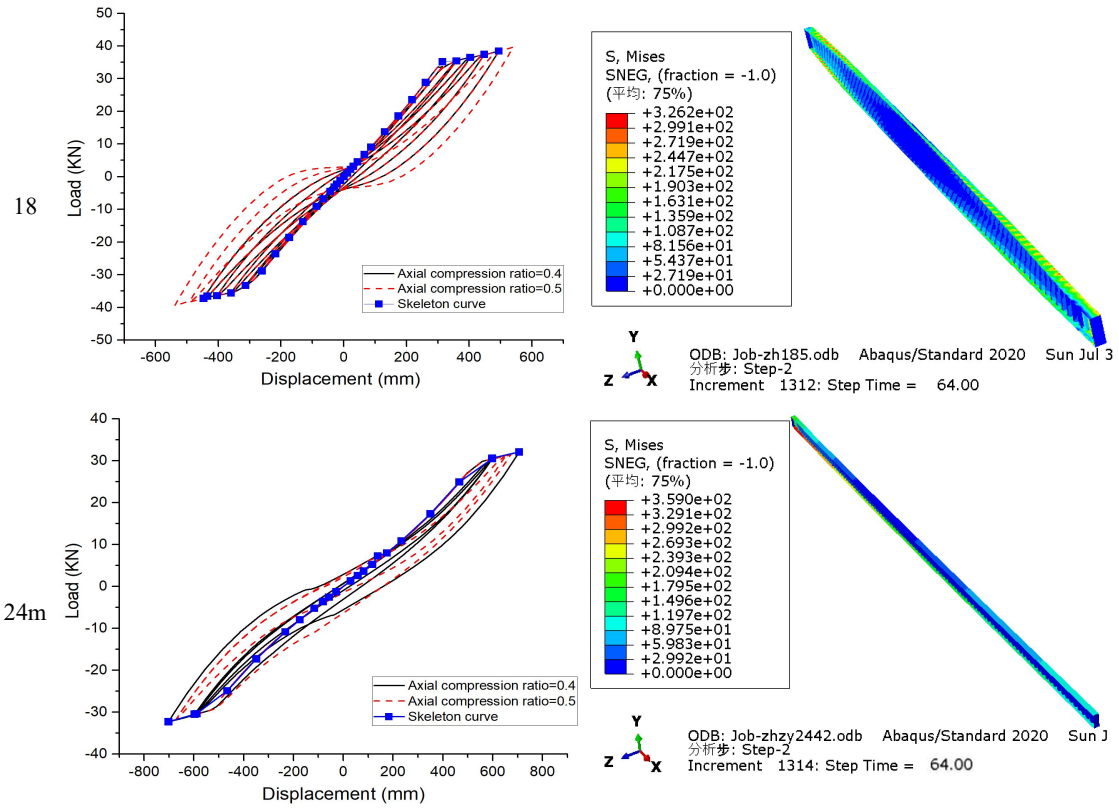

To sum up, the following conclusions are drawn:

1. The rigid frame beam span of 6-24m can meet the rare earthquake of 8 degrees or less, and the 18m and 24m span can meet the rare earthquake of 9 and below at the same time, so it is necessary to control the beam span reasonably to ensure that the structure has better seismic resistance.

2. To ensure that the structural failure is always in the elastic stage, and the axial compression ratio should not be too large when the structural design is reasonable, the corrugated web rigid frame structure can be used in the rare seismic intensity area above 7 degrees when the axial compression ratio is 0.5.

3. The axial compression ratio has little influence on the hysteretic performance of the members. With the increase of the span, the members will slip, the hysteretic curve will shrink, and the energy dissipation will become smaller, which is not conducive to the earthquake resistance of the structure.

Reference:

[1]Chen Haoyu. Analysis and Discussion on the Application of Prefabricated Design and Construction in Green Buildings [J]. China Residential Facilities, 2023 (06): 37-39

[2]IBRAGIMOV A, ZINOVEVA E, ROSINSKIY S. Prefabricated steel structures with a corrugated web (Part 1. Beam)[J/OL]. IOP Conference Series: Materials Science and Engineering, 2020, 869(7): 072041.

[3]ZHAO Q, QIU J, ZHAO Y, et al. Performance-Based Seismic Design of Corrugated Steel Plate Shear Walls[J/OL]. KSCE Journal of Civil Engineering, 2022, 26(8): 3486-3503.

[4]Feng Wen, Liu Baodong, Mou Kai, etc. Study on Seismic behavior of continuous rigid frame Bridge with corrugated Steel webs [J]. Earthquake resistance and strengthening of engineering, 2015 74.DOI:10.16226/j.issn.1002 37 (05): 70-seismic-8412.2015.05.012.

[5]Li Pengfei, Liu Baodong, Xiao Yingnan. Influence of pier types on dynamic characteristics of continuous rigid frame bridge with corrugated steel webs [J]. Bridge Construction, 2011 (02): 27-29.

[6]]Wan Yu.Seismic performance analysis of H-shaped steel cantilever beam and frame with corrugated web [D].

Nanchang University, 2022.DOI:10.27232/d.cnki.gnchu.2022.002363.

[7]Peng Jiacheng. Theoretical and experimental study and damping effect analysis of corrugated steel web damper [D]. Huazhong University of Science and Technology 2020.DOI:10.27157/d.cnki.ghzku.2020.005773.

[8]MOU X, LV H, LI X. Seismic performance of corrugated steel plate composite shear walls with various configurations[J].

[9]Technical Specification for Application of Corrugated Web Steel Structures (CECS 291:2011) [S] China Planning Press. 2011

[10]Technical Specification for Steel Structures of Lightweight Buildings with Portal Frames (CECS102:2010) [S]. Beijing: China Planning Press

[11]Cheng Jin Analysis on overall stability performance of H-shaped steel axial compression members with corrugated webs [D]. Southwest Petroleum University, 2017

[12]Md S, Carla D, Thomas T. Experimental investigation of the hysteretic behavior of single-story single- and coupled-panel CLT shear walls with nailed connections[J]. Engineering Structures,2023,291.

[13]Hu Yuxian, Earthquake Engineering [M], Beijing, Earthquake Press, 1988: 133 ～ 16

[14]Technical Specification for Steel Structures of Lightweight Buildings with Portal Frames (CECS102:2010) [S]. Beijing: China Planning Press

[15]HU Qi Study on the seismic performance of coupling beam in coupled shearwall [D]. Hefei: Hefei University of Technology2013: 1-4.(in Chinese)

[16]HANXiaolei. Study on the structural control performance of coupled shear walls with a stiffening beam [D]Guangzhou: South China University of Technology1991: 2. (in Chinese)

[17]CHEN Xuewei. Research on deformation limits the state of components of shear-wall structure and development of the computing platform [D]. Guangzhou: South China University of Technology, 2011: 160. (in Chinese)

[18]LIANG Oizhi，HANXiaolei. Performance of stiffening coupling beam unconventional coupling beam under low-frequency cyclic load [J] .Journal of South China University ofTechnology (Natural Sciences) , 1995 , 23(1) : 27-33(in Chinese)

[19]FEMA. Prestandard and commentary for the seismic rehabilitation of buildings: FEMA 356[S]Washington DC: Federal EmergencyManagementAgency，2000.

[20]Wang Mingqing, Zhang Zhi, Chen Zhenhai, et al. Seismic performance analysis of a new type of connection node between embedded wall panels and steel frames [J]. Science and Technology and Engineering, 2023,23 (18): 7868-7877
[21]XUE G, BAO W, JIANG J, et al. Hysteretic Behavior of Beam-to-Column Joints with Cast Steel Connectors[J/OL]. Shock and Vibration, 2019, 2019: 1-20.
[22]Zhang Li, Xu Yafeng Analysis of the Influence of Different Axial Compression Ratios on the Hysteretic Performance of Carbon Fiber Reinforced Steel Reinforced Concrete Filled Steel Tubular Columns [C]//Shenyang Municipal Party Committee, Shenyang Municipal People's Government. 2011:6
[23]Lv Liang, Sun guo-hua, Yang Weixing. Analysis of the influence of axial compression ratio on the hysteretic performance of high-strength concrete composite shear walls with I-shaped steel tube bundles [J]. Journal of Suzhou University of Science and Technology (Engineering Technology Edition), 2023,36 (01): 8-14